J Solid State Electrochem (2011) 15:479–484
DOI 10.1007/s10008-010-1104-y

ORIGINAL PAPER

Microfabrication of thermoelectric modules by patterned electrodeposition using a multi-channel glass template

Da-Wei Liu · Jing-Feng Li

Received: 10 February 2010 / Revised: 10 May 2010 / Accepted: 12 May 2010 / Published online: 26 May 2010

Abstract A microfabrication process has been developed to elaborate microscale thermoelectric modules with high-aspect-ratio pillars assembled in a glass micromold, whose multi-channels are formed by combining mechanical machining and hot-pressing processes. This paper describes how to fill the multi-channel glass molds with thermoelectric materials by introducing a patterned electrochemical deposition method, in which a deposition cathode with two series of interdigital electrodes is designed. A reverse-pulsed electrodeposition method is found effective to overcome the difficulty for deep-filling that is required for fabricating thermoelectric pillars with high aspect ratios. A pulse circle of −200 mV for 4 s, +500 mV for 1 s, and 0 mV for 3 s (vs. saturated calomel electrode) was determined for preparing N-type Bi_2Te_3 arrays with a high aspect ratio exceeding ten from a solution containing 0.0075 M Bi^{3+} and 0.01 M $HTeO_2^+$. The as-deposited pillars show reasonable electrical resistivity as compared with common bulk Bi_2Te_3 materials.

Keywords Thermoelectric module · Microfabrication · High aspect ratio · Patterned electrodeposition · Bi_2Te_3

Introduction

Shrinking feature sizes is becoming a top issue for today's integrate cricuit (IC) and microelectromechanical systems technology. Thermoelectric devices, which can work either in "Seebeck effect" and "Peltier effect" model, are thought to be the most promising candidates as micro-transfer components for thermal and electric energy [1–3]. That is because thermoelectric devices that work without any moving parts can be easily miniaturized for the integration into micro-systems [4–8]. As reported, thermoelectric micro-devices can be utilized as micro-sensors and temperature stabilizers [5, 6] or can be used as energy resources for micro-systems [7, 8].

A typical thermoelectric device comprises couples of P- and N-type pillars that are connected electrically in series. How to reduce the size and increase the conversion output power and efficiency are the critical topics to realize the applications of thermoelectric components to micro-systems. Because higher output power and efficiency can be achieved with a larger temperature difference, increasing the aspect ratio of thermoelectric pillars is a direct way to enhance the thermoelectric performance when the thermoelectric materials for the device are already chosen [9].

Conventionally, thermoelectric elements are prepared by mechanically dicing thermoelectric bulk materials. Because most thermoelectric materials are mechanically weak, conventional mechanical machining has its limitation to miniaturization. Many efforts have been made to develop the fabrication technology of micro-thermoelectric pillars. In recent years, the molding method, which is filling P- and N-type thermoelectric materials alternately into molds with micro-channel arrays to make thermoelectric modules, has attracted much attention [2, 3, 6, 8]. With the molding method, miniaturization can be much easier, and some groups have developed their ways of fabricating thermoelectric micro-devices, such as alumina nano-templates and polymer templates filled by electrodeposition [2, 3, 10] and RIE (reactive ion etching)-etched silicon micro-templates filled by powder hot-pressing [8]. However, neither

D.-W. Liu · J.-F. Li (✉)
State Key Laboratory of New Ceramics and Fine Processing,
Department of Materials Science and Engineering,
Tsinghua University,
Beijing 100084, China
e-mail: jingfeng@mail.tsinghua.edu.cn

alumina nor polymer templates can be made very thick to achieve high aspect ratios unless using the expensive LIGA technology. Although RIE-derived silicon templates can solve this problem, a template-removing process is required after filling because the thermal conductivity of silicon is so high that will reduce the energy conversion efficiency. In the present work, we developed a low-cost glass molding method. Since the glass template is low in thermal conductivity and electrically insulting, it can be retained even after having been filled. Therefore, using a glass mold not only simplifies the fabrication process but also helps to enhance the rigidity of thermoelectric modules. Nevertheless, the point is the mold-filling process, for which an electrodeposition method was considered to be suitable because it is an environmental-friendly and IC-compatible technology.

The thermoelectric materials we chose for electrodeposition are Bi-Sb-Te system (Bi_2Te_3 for N type and $Bi_{0.5}Sb_{1.5}Te_3$ for P type) because of their good room temperature thermoelectric performances that are preferred by micro-devices [11]. Although the electrodeposition of Bi-Sb-Te system materials have been studied for several years, the reported works are mainly focused on films or nanowires [12–16]. The electrodeposition of high aspect ratio and large-scale (about 1 mm high) array is still a challenging topic for most thermoelectric materials. In the present work, we focus our attention on the study of Bi_2Te_3 (N type) into the glass templates.

Experimental procedures

Designation of glass molding and patterned electrodeposition process

The whole fabrication processes for thermoelectric micro-devices are shown in Fig. 1a–i. About ten to 20 flutes are mechanically scored on glass slices 150 μm in thickness (Fig. 1a) by a commercial automatic cutting machine (ZSH306D, Shenyang, China). The flutes are about 30 μm in width and 70 μm in depth and separated by about 120 μm. In the next step, several slices with flutes are piled up and localized perpendicularly with a homemade clamp, and then they are heated up to 600 °C for 2 h in a furnace with mechanical constraint from top and bottom (Fig. 1b). During sintering, the glass slices join with each other in the contacted area, and a template with straight channels forms (Fig. 1c). The as-fabricated template is about several centimeters in length, which is too large for a thermoelectric micro-device. The template is then cut into required length (about 1 mm) by the cutting machine as mentioned (Fig. 1d). After that, the substrate-free glass template has been made. The electrodeposition electrodes are then made on a silicon wafer by photolithograph and patterned magnetron sputtering, as shown in Fig. 1e. The electrodes are a series of interdigital metal lines (two groups of parallel electrode lines that are connected with each other in one end), which are a little wider than the channels of the glass template. In each group, the distance between each line is twice as large as the distance between two channels on the glass template. The two groups of electrode lines just correspond to the positions of channels on the glass template that will be filled with P- or N-type thermoelectric materials. After that, the substrate with electrodes is assembled and welded with the glass template using metal–glass bonding technology [17] (Fig. 1f).

The next process is filling the template with P- and N-type thermoelectric materials alternatively, which takes two steps of electrodeposition. P- or N-type materials are electrodeposited from two baths of electrolytes separately by controlling which group of electrodes is connected to the cathode (Fig. 1g–h). This method is suitable for electrodeposition because the elements only get crystallized from ions and grows where the electrons can be provided. After filling, the last step is to remove the substrate by mechanical polishing and to make the connection electrodes for the thermoelectric module on both top and bottom sides of the template by photolithograph and patterned magnetron sputtering (Fig. 1i).

Electrodeposition of Bi_2Te_3 into glass templates

The schematic illustration of electrodeposition cathode is shown in Fig. 2a; silver paste is used as both an electrically conducting layer and adhesive between the template and substrate. In order to control the cathodic current precisely, we use melted paraffin to cover the entire exposed electrical conductive surface on the cathode. A stirrer is used to enhance the mass transfer of ions during electrodeposition. The electrolyte contains 0.0075 M Bi^{3+} and 0.01 M $HTeO_2^+$, and all other cell conditions are consistent with our previous work [18].

The morphologies of the deposits are investigated by using both optical microscopy and scanning electron microscopy (SEM). The phase structure is examined by X-ray diffraction (R-Axis Spider, Rigaku, Japan). The *I-U* plot of a single pillar is measured by contacting two micro-probes (10 μm in diameter at tip) on each end of the pillar from cross-section and with a PC-controlled voltage source and ammeter.

Results and discussions

The glass template that fabricated with the method mentioned above is shown in Fig. 3. Glass slices are well welded to each other without any crack after bonding, and the channel array

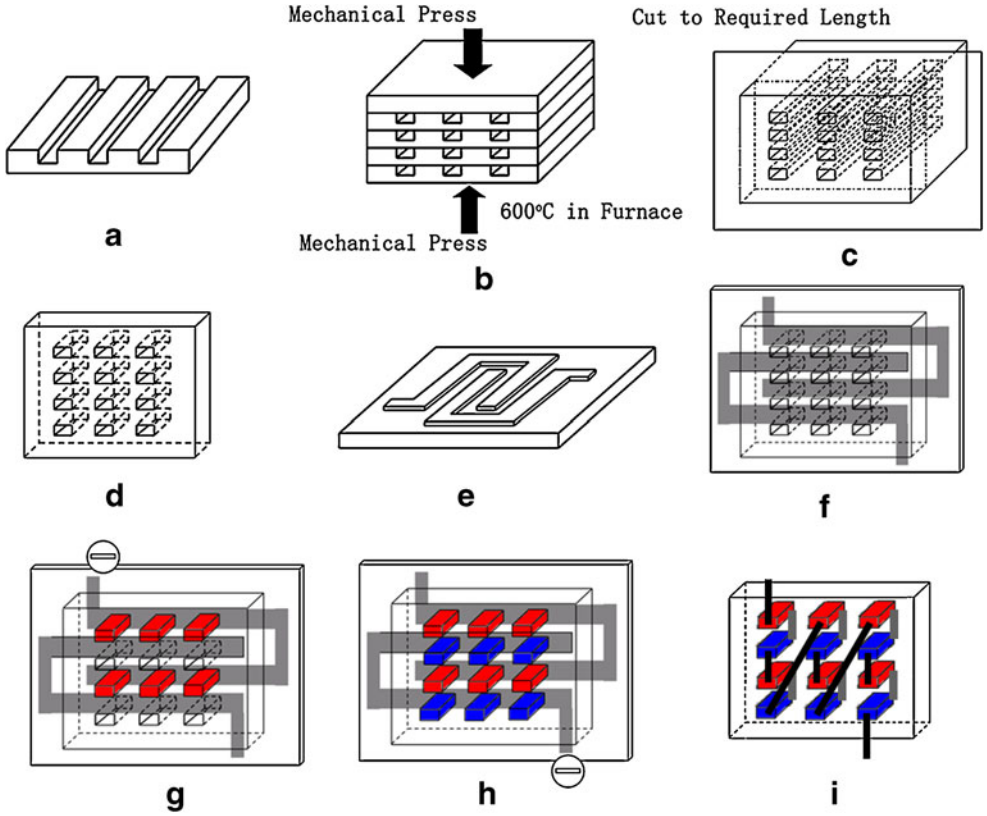

Fig. 1 Schematic illustration of the fabrication process for thermoelectric micro-modules: make flutes on glass slices by cutting (**a**), pile up and sinter the glass slices with press from top and bottom (**b**), cut the as-sintered glass template into required length (**c**, **d**), magnetron sputter the deposition electrodes on a silicon wafer (**e**), bond the template with the wafer (**f**), electrodeposit N-type thermoelectric array with one half of the interdigital electrodes connected to the cathode (**g**), electrodeposit P-type thermoelectric array with the other half of the interdigital electrodes connected to the cathode (**h**), remove the substrate wafer and make the connection electrodes for the thermoelectric device on both top and bottom side of the template (**i**)

is formed as designed. In a cross-section area of 1×3 mm, about 50 micro-channels can be fabricated for molding.

Although DC or on–off pulsed current/potential electric source can successfully deposit Bi_2Te_3 thin films or nanowires, it fails to fill microscale array with high aspect ratios. Under the same deposition condition used for fabricating films, only a few channels can be filled even after a very long time (over 60 h). With more negative potentials, electrodeposition is much faster, but the channels are all poorly filled with large and roughly grown grains. On–off pulsed deposition also could not improve the filling quality. This trouble is caused by the strong dilution of ion concentration C_{hi} in high-aspect-ratio channels, as shown in Fig. 2a. Because the channels are very deep and narrow, contra-flow and three-dimensional diffusion inside are suppressed, and one-dimensional diffusion is the only way to transfer the ions for deposition [19–21]. In this way, the ion concentration gradient near the cathode is very large, which causes the dendritic growth of Bi_2Te_3 during the electrodeposition [18]. That is why the templates cannot be well-filled with large constant currents.

To reduce the intensive ion dilution near the cathode, a reversed pulse has been introduced in addition to the on–off pulsed potential, as shown in Fig. 2b (three cycles). Such a modification is proved to be very effective relative to normal on–off pulsed electrodeposition since the ion concentration gradient can be released greatly by reversed pulse. Previous studies show that Bi_2Te_3 begins to deposit from solution when the cathode potential is negative than −40 mV and dissolves around +500 mV [18]. According to that, one cycle is divided into three steps: deposition (−200 mV, 4 s), dissolving (+500 mV, 1 s), and off (0 mV, 3 s). At the dissolving step, the as-deposited Bi_2Te_3 partly dissolves into the solution. Consequently, the as-dissolved ions increase the ion concentration near the cathode, which helps to release the ion concentration gradient and provides more evenly distributed ions for the next deposition step [19, 20]. In addition, if some columns grow faster than others during the previous deposition step, they will also dissolve faster in the following reversed step. This is because higher deposition speed leads to stronger dilution, which increases the reaction rate of dissolving. Therefore, the inhomogeneity in Bi_2Te_3 columns is reduced during the dissolving step. In Fig. 2b, the response current of each step is the same within different cycles from the beginning, which suggests that the ion concentration gradient is almost released during the dissolving and off steps.

The filling results are shown in Fig. 4, in which *a* is from top view under an optical microscope right after the deposition, *b* and *c* are from top view by SEM after surface polishing, and *d* is from cross-section view by SEM. The black "caps" in Fig. 4a are the deposits that grow out of the pores, which show that most of the channels were filled up after electrodeposition. Some channels at the fringe of the

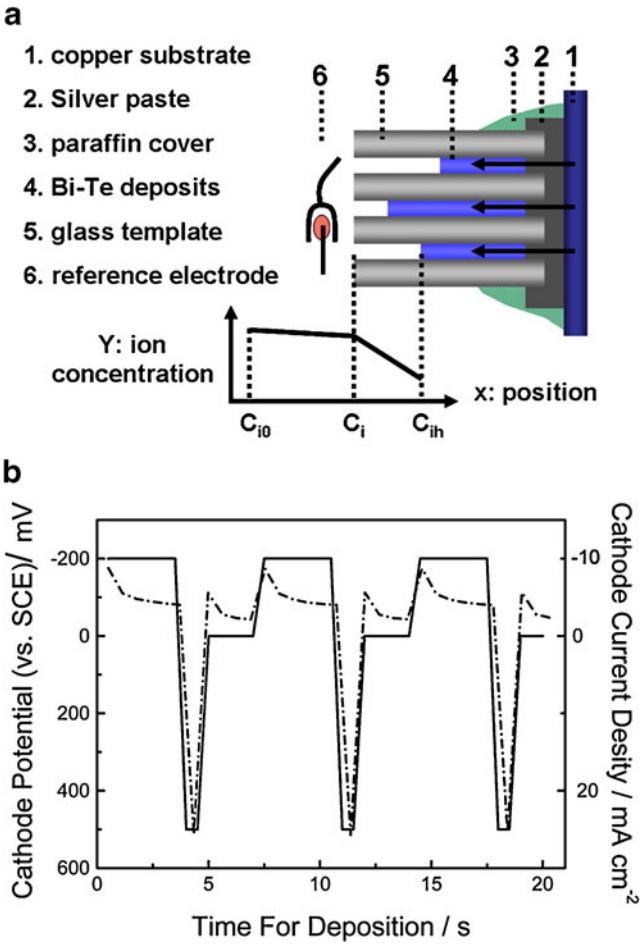

Fig. 2 The cathode of electrodepositing Bi_2Te_3 array: the schematic illustration (**a**), and the record of cathode potential (*solid line*) and response current density (*dot line*) during reversed-pulsed electrodeposition (**b**)

template were not filled by the deposition probably because they were unintentionally covered with paraffin when fabricating the cathode; we will improve it in the future. Moreover, the sizes of the "caps" are almost the same, which suggests that the filling process of each channel is almost finished synchronously. After mechanically polishing the top surface, the deposits "caps" are removed, leaving a dense and smooth surface of Bi_2Te_3 deposits, as shown in Fig. 4b, c. The cross-section morphologies in Fig. 4d show that the template has been well filled-up with nano-scale polycrystal Bi-Te deposits. However, preparing a cross-section sample is very difficult because Bi_2Te_3 is much softer and weaker than the glass template due to its layered crystal structure [1, 12]. As a result, a few deposits fell from the template as shown in Fig. 4d during the polishing process. That is, the defect-like points observed in Fig. 4d should be "artificial".

The EDS results show that the deposits inside channels from bottom to top are comprised of $Bi_{(1.85–1.95)}Te_3$ alloys, whose element ratios are very close to Bi_2Te_3. The composition variation in deposits ($[Bi] = 1.85 \sim 1.95$) is caused by the small shifting of C_{Bi}/C_{Te} ratio at the interface between solution and deposits during deposition. In fact, in a longer unfilled channel, the ion concentration drops more quickly during the cathodic pulse. Therefore, the average C_{ih} (as in Fig. 2a) within each cathodic pulse increases when the channel is gradually filled-up. Since the diffusion rates of $[Bi^{3+}]$ and $[HTeO_2^+]$ are different, an increase in C_{ih} will result in the shifting of C_{Bi}/C_{Te} ratio. The phase structure of the deposits is shown in Fig. 5. The peak-packet near $2\theta = 30^o$ represents the glass template, and other sharp peaks identify the existence of Bi_2Te_3.

The *I-U* plot of a single pillar is shown in Fig. 6. A linear fit of the data shows a slope coefficient (k) of 0.086 with an error (e) of 9.1×10^{-5}, which can deduce a resistance (R) of 11.6 Ω for the micro-pillar. If calculated with a resistivity of 1×10^{-5} (as common Bi_2Te_3 dense bulks), the pillar with 0.85 mm in length and 30×70 μm in cross-section has a resistance of 4.05 Ω, which is comparable to the measured

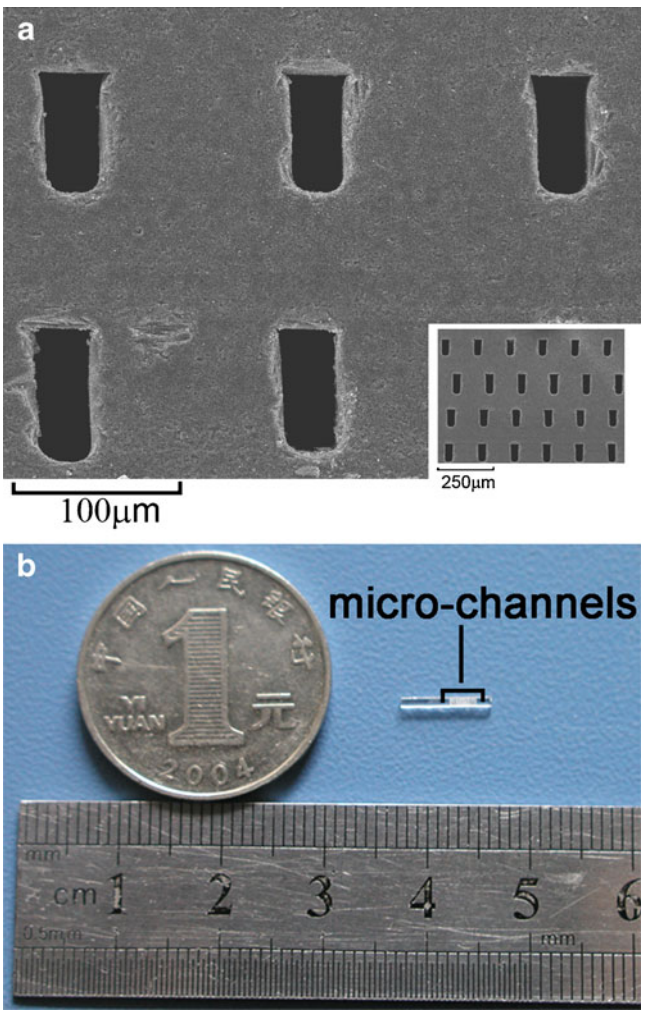

Fig. 3 The glass template: from *top view* under SEM with different magnification (**a**) and in real scale (**b**)

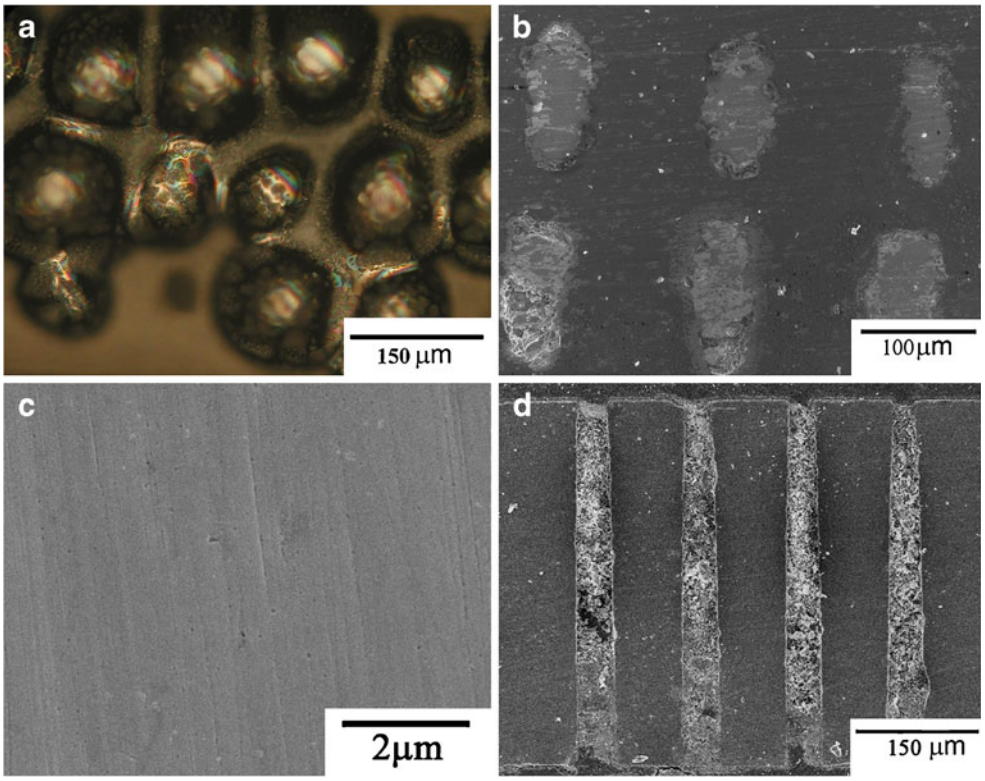

Fig. 4 The micrograph of a glass template after filling by reversed-pulsed electrodeposition: from top view under optical microscope (before polishing) (**a**), from top view under SEM (after polishing) (**b**), under SEM with high magnification (**c**), and from cross-section view under SEM (**d**)

value in consideration of the resistances of contacting areas and probes.

The above results demonstrate that miniaturized thermoelectric modules with high-aspect-ratio Bi_2Te_3 micro-pillars can be fabricated by patterned electrodeposition into a multi-channel glass template. A similar procedure can be also applied to the fabrication of P-type Bi-Sb-Te alloy micro-pillars, which can be filled into the alternative lines of channels, as shown in Fig. 1h. Although more efforts are required to accomplish the whole process for manufacturing the modules, the present study shows that the key problems were already resolved.

Conclusion

We have proposed a glass molding and electrodeposition method for fabricating thermoelectric micro-modules with high-aspect-ratio thermoelectric pillars. The present study firstly showed how to make multi-channel glass micro-

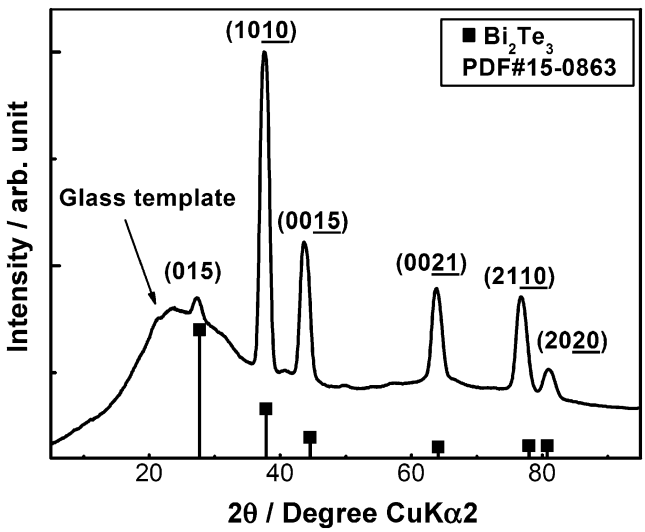

Fig. 5 X-ray diffraction pattern of filled templates from top view

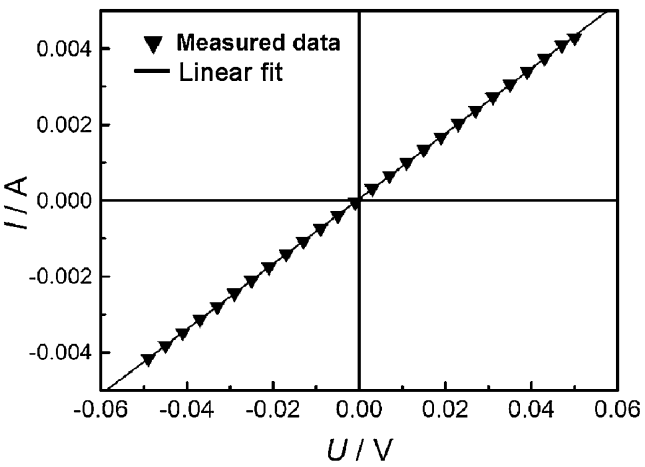

Fig. 6 *I-U* plot of a single pillar (*inverted filled triangle*) that measured from cross-section with two probes, and a linear fit of the data (*straight line*)

molds by combining mechanical cutting and hot-pressing. By using this technique, glass micro-channel templates with arbitrary high aspect ratios were facilely prepared even without use of deep reactive ion etching as required for silicon micro-molding process. This study also found a reverse-pulsed electrodeposition to fill the micro-channels in the glass micro-molds with Bi_2Te_3 compound thermoelectric materials. It was confirmed that the filled arrays have a chemical composition close to the designed Bi/Te ratio, which also shows reasonable electrical properties.

Acknowledgments This work was supported by the Ministry of Science and Technology of China (Grant no. 2007CB607505) and National Nature Science Foundation (Grant no. 50820145203).

References

1. Rowe DM (1995) CRC handbook of thermoelectrics. CRC, Washington D.C
2. Snyder GJ, Lim JR, Huang CK, Fleurial JP (2003) Nat Mater 2:528–531
3. Lim JR, Whitacre JF, Fleurial JP, Huang CK, Ryan MA, Myung NV (2005) Adv Mater 17:1488–1492
4. Disalvo FJ (1999) Science 285:703–706
5. Izaki R, Kaiwa N, Hoshino M, Yaginuma T, Yamaguchia S, Yamamoto A (2005) Appl Phys Lett 87:243508–243510
6. Itoigawa K, Ueno H, Shiozaki M, Toriyama T, Sugiyama S (2005) J Micromech Microeng 15:S233–S238
7. Goncalves LM, Couto C, Alpuim P, Correia JH (2008) J Micromech Microeng 18:064008–064012
8. Li JF, Tanaka S, Umeki T, Sugimoto S, Esashi M, Watanabe R (2003) Sens Actuators A 108:97–102
9. Glatz W, Schwyter E, Durrer L, Hierold C (2009) J Microelectromech Syst 18:763–772
10. Wang W, Jia FL, Huang QH, Zhang JZ (2005) Microelectron Eng 77:223–229
11. Poudel B, Hao Q, Ma Y, Lan YC, Minnich A, Yu B, Yan X, Wang DZ, Muto A, Vashaee D, Chen XY, Liu JM, Dresselhaus MS, Chen G, Ren Z (2008) Science 320:634–638
12. Tittes K, Bund A, Plieth W, Bentien A, Paschen S, Plotner M, Grafe H, Fischer WJ (2003) J Solid State Electrochem 7:714–723
13. Heo P, Hagiwara K, Ichino R, Okido M (2006) J Electrochem Soc 153:C213–C217
14. Yoo BY, Huang CK, Lim JR, Herman J, Ryan MA, Fleurial JP, Myung NV (2005) Electrochim Acta 50:4371–4377
15. Michel S, Diliberto S, Stein N, Bolle B, Boulanger C (2008) J Solid State Electrochem 12:95–101
16. Lee J, Farhangfar S, Lee J, Cagnon L, Scholz R, Gosele U, Nielsch K (2008) Nanotechnology 19:365701–365708
17. Liu C (2006) Foundations of MEMS. Pearson Education Inc., New Jersey
18. Liu DW, Li JF (2008) J Electrochem Soc 155:D493–D498
19. Dixit P, Miao JM (2006) J Electrochem Soc 153:G552–G559
20. Chandrasekar MS, Pushpavanam M (2008) Electrochim Acta 53:3313–3322
21. Yang H, Chein RY, Tsai TH, Chang JC, Wu JC (2006) Microsyst Technol 12:187–192